Stillwater Model Dam line D1P2NO24 P-wave refraction, 100 WET iterations @30Hz using wavepath width 30 percent and Ricker wavelet for back-projection of residuals

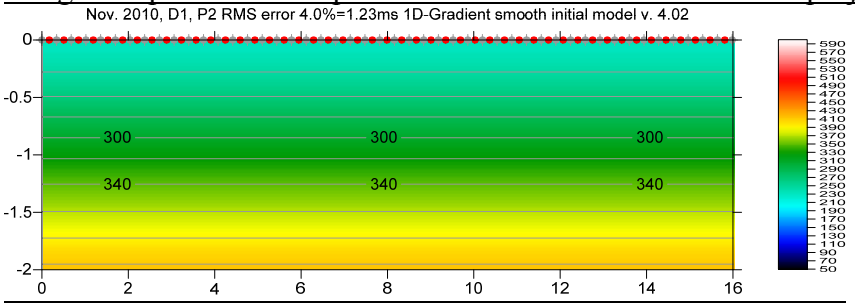

Fig. 1 : 1D-gradient starting model obtained with *Smooth invert|WET with 1D-gradient initial model*. Default settings. *Grid cell size* forced to 0.04m in *Header|Profile* (Fig. 7). Red circles are sources. Grey symbols are geophones.

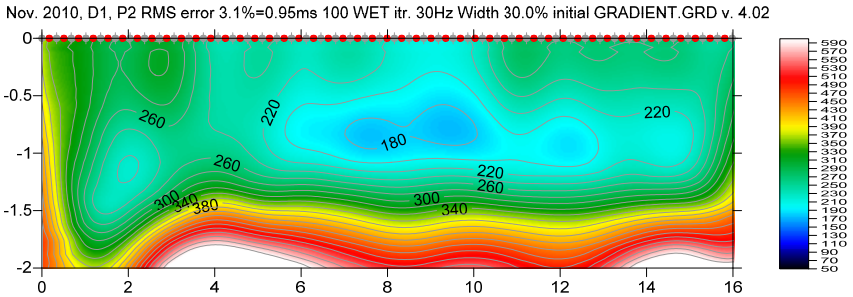

Fig. 2 : 100 WET iterations, WET frequency 30Hz, Wavepath width 30%. Starting model is Fig. 1. Ricker differentiation 0. Minimal WET smoothing. Don't adapt shape of filter. See Fig. 5. No WDVS smoothing.

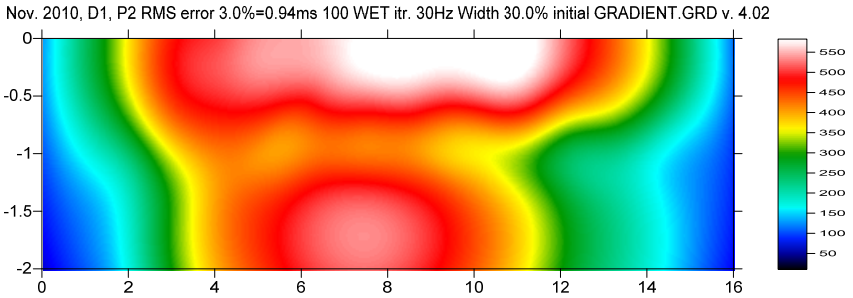

Fig. 3 : WET wavepath coverage plot obtained with Fig. 2. Unit is summed wavepath weight squared. Wavepath coverage plot is sharpened with ***Raise wavepath weight to power*** = 2.0. See Fig. 8.

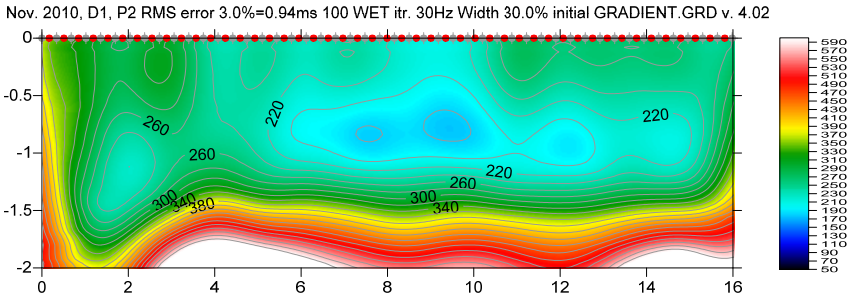

Fig. 4 : Same WET inversion as Fig. 2 but with WDVS smoothing activated @600Hz (Fig. 6).

We reprocessed the original data used for Stillwater Model Dam Fig. 3.13 in PhD Thesis Leti Wodajo (Wodajo, 2018) to better image two constructed low-velocity regions in the dam.

Compare our optimized interpretation in Fig. 4 with Fig. 3.13 (Wodajo, 2018). While Fig. 3.13 was obtained with default ***WET frequency*** 50Hz and default ***wavepath width*** 5%, we lowered the WET frequency to 30Hz and increased the wavepath width to 30% (Fig. 5). Also we changed the ***Ricker differentiation*** from default -1 (Gaussian) to 0 (Ricker wavelet; Schuster 1993).

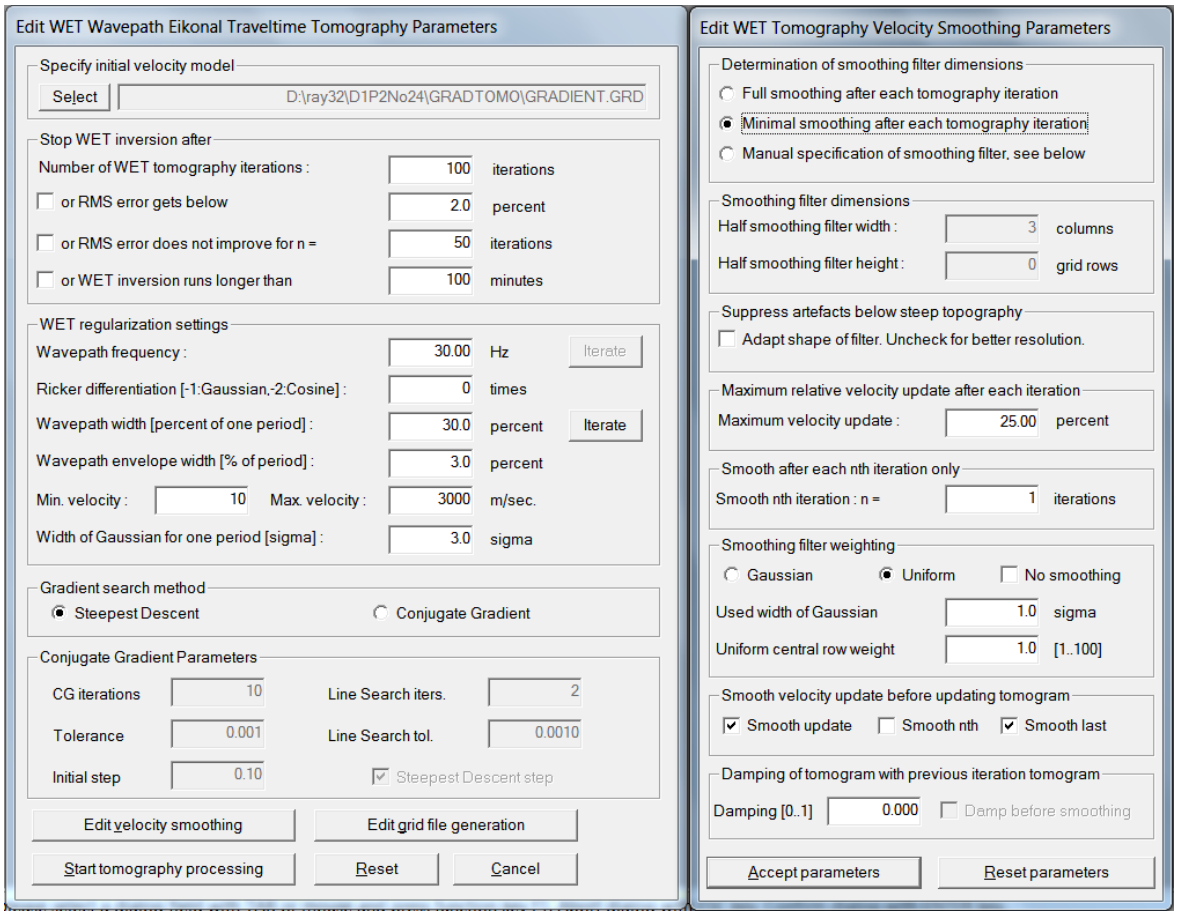

Fig. 5 : *WET Tomo|Interactive WET* main dialog (left). *Edit velocity smoothing* (right).

We sharpened the ***Wavepath coverage plot*** (Fig. 3) with ***Raise wavepath weight to power*** = 2.0 (Fig. 8) to optimally visualize and match low-velocity anomalies (Fig. 2 and Fig. 4) on the coverage plot.

We used the default 1D-gradient starting model (Fig. 1) obtained by laterally averaging the DeltatV pseudo-2D velocity (Sheehan, 2005). We used optimized WET inversion settings and smoothing as in Fig 5. When enabling ***Wavelength-Dependent Velocity Smoothing*** (WDVS; Zelt and Chen 2016; Rohdewald, 2021a; Rohdewald, 2021b) at 600Hz (Fig. 6) for WET inversion the two central low-velocity zones get separated horizontally more clearly (Fig. 4).

We set ***Ricker differentiation*** to 0 (Fig. 5) using a Ricker wavelet for weighting of WET velocity update across the wavepath during back-projection of residuals (Schuster, 1993). Ricker wavelet weighting works better than default Gaussian update weighting (Ricker differentiation = -1) for this line.

Before running our WET inversion (Fig. 5) also check option ***Model|Forward modeling Settings|Normalize RMS error with maximum picked time*** to be compatible with RMS error display on top of Fig. 3.13 (Wodajo, 2018) obtained with version 3.20 of our software.

For this line we observed that the lower the WET ***Wavepath frequency*** and the wider the WET ***Wavepath width*** (Fig. 5) the deeper the low-velocity zone in center of tomogram is imaged. This ***dependence of imaged anomaly depth on WET wavepath frequency and width*** confirms that you need a-priori information about the depth of low-velocity zones for optimal interpretation with our WET inversion (Wodajo, 2018). Also this dependence on WET parameters reconfirms that SRT interpretation is non-unique especially in case of decreasing velocity with increasing depth.

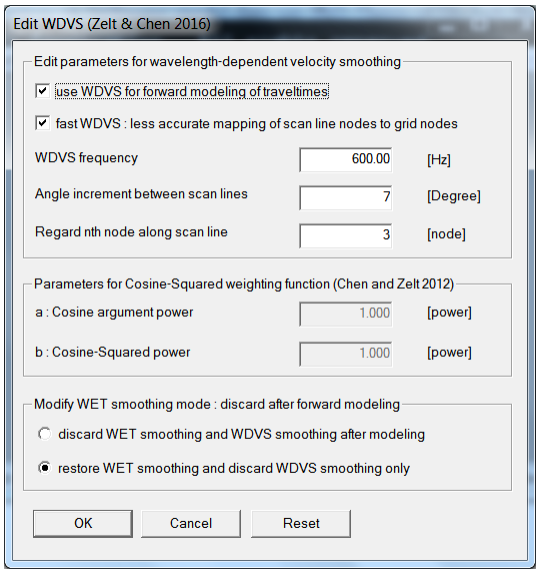

Fig. 6 : *Model|WDVS Smoothing*

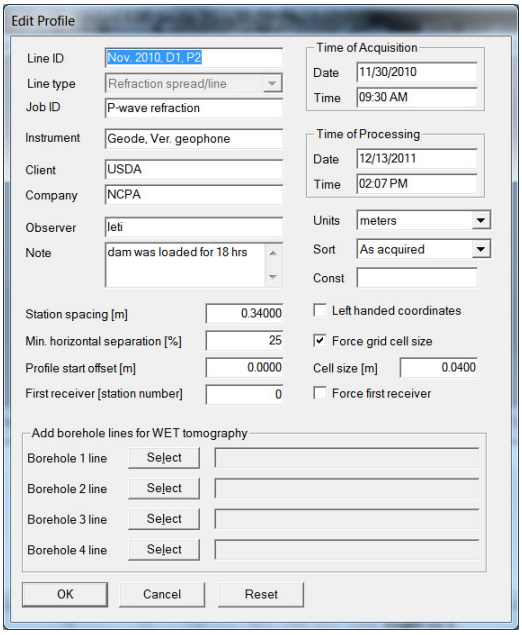

Fig. 7 : *Header|Profile*

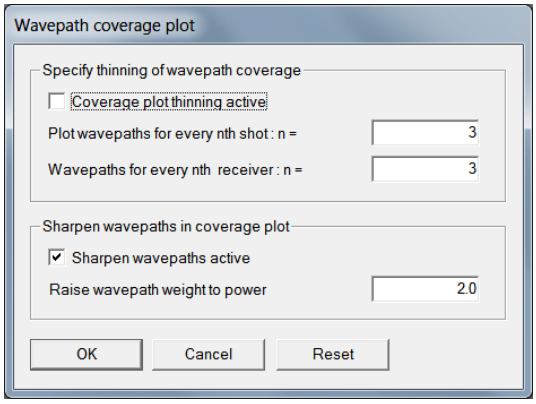

Fig. 8 : *WET Tomo|Coverage plot setup*

The profile database is available at https://rayfract.com/tutorials/D1P2No24_seis32_50ms_July21_2021.rar

- download above .rar archive to your hard disk
- open Windows Explorer
- navigate into your download directory
- select the .rar archive with left mouse button
- right-click the selected .rar archive and select "Copy" command
- in Windows Explorer navigate into your **C:\RAY32** root directory
- click “New folder” and create a new directory **C:\RAY32\D1P2NO24**
- navigate into this new folder by left-clicking it
- paste above .rar archive with "Paste" command in Windows Explorer “Organize” menu
- right-click the .rar archive in your **C:\RAY32\D1P2NO24** directory and select "Extract here" command
- start up Rayfract® via desktop icon
- select ***File|Open Profile*** and **C:\RAY32\D1P2NO24\SEIS32.DBD**

- see our download instructions for details on usage of Windows Explorer and how to get started with our tutorials.

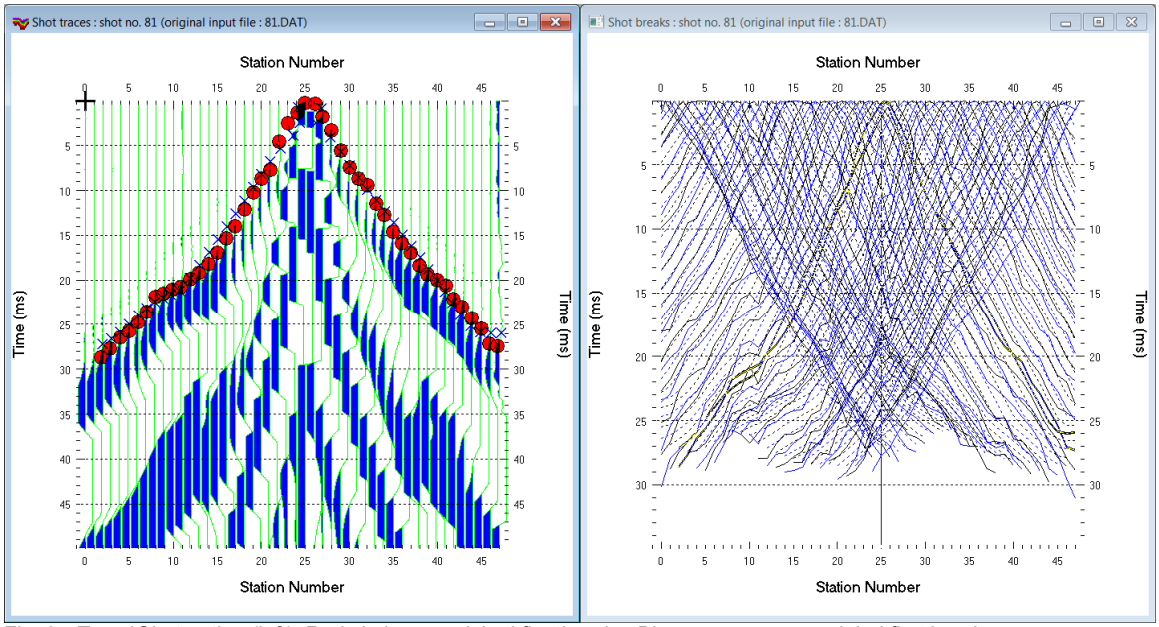

Fig. 9 : *Trace*|*Shot gather* (left). Red circles are picked first breaks. Blue crosses are modeled first breaks. *Refractor*|*Shot breaks* (right). Solid grey&blue curves are picked traveltimes. Dashed blue curves are modeled times.

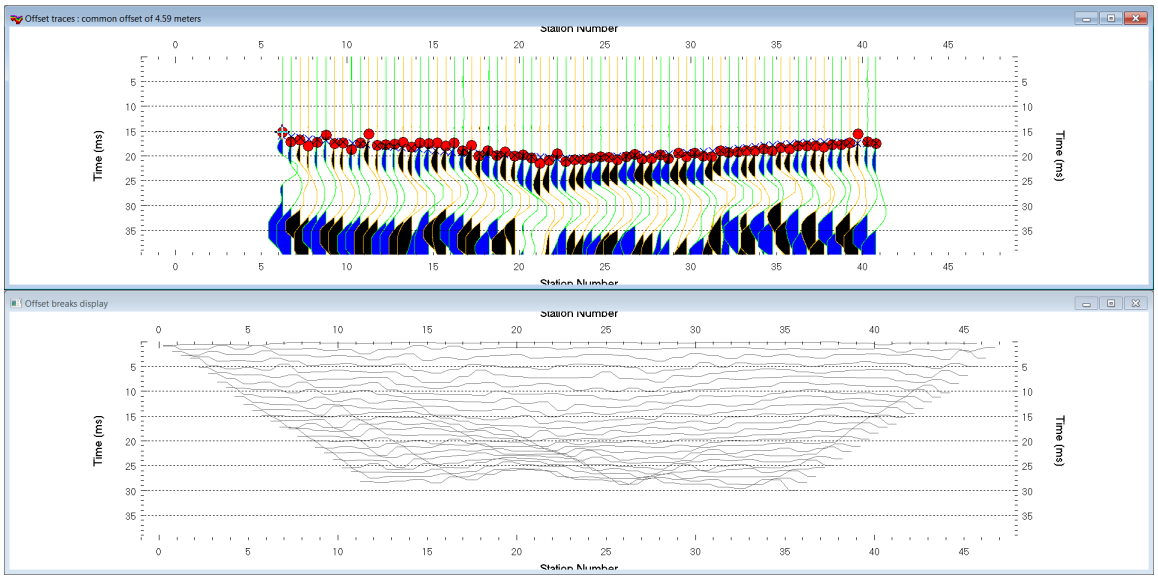

Fig. 10 : *Trace*|*Offset gather* for common offset of 4.59 meters (top). *Refractor*|*Offset breaks* (bottom).

References

Bakhtiari Rad, P, Rohdewald, S.R.C., 2021. Tunnel detection using Frequency-Dependent Traveltime Tomography. The National Center for Physical Acoustics at University of Mississippi.

Rohdewald, S., Burton, B., Sheehan, J., Doll, W., 2010, Processing of seismic refraction tomography data, SAGEEP short course notes, Keystone, Colorado, https://rayfract.com/SAGEEP10.pdf.

Rohdewald, S.R.C. 2021a, Improving the resolution of Fresnel volume tomography with wavelength-dependent velocity smoothing, *Symposium on the Application of Geophysics to Engineering and Environmental Problems Proceedings* : 305-308. https://doi.org/10.4133/sageep.33-169

Rohdewald, S.R.C. 2021b, Improved interpretation of SAGEEP 2011 blind refraction data using Frequency-Dependent Traveltime Tomography, EGU General Assembly 2021, online, 19–30 Apr 2021, EGU21-4214, https://doi.org/10.5194/egusphere-egu21-4214 .

Schuster, G.T., Quintus-Bosz, A., 1993, Wavepath eikonal traveltime inversion: Theory. Geophysics, Volume 58, 1314-1323.
Sheehan, J.R., Doll, W.E., Mandell, W., 2005, An evaluation of methods and available software for seismic refraction tomography analysis, JEEG, Volume 10(1), 21-34.
Watanabe, T., Matsuoka, T., Ashida, Y., 1999, Seismic traveltime tomography using Fresnel volume approach, SEG Houston 1999 Meeting, Expanded Abstracts.
Wodajo, L.T. 2018, Integrity Assessment Of Earthen Dams And Levees Using Cross- Plot Analysis Of Seismic Refraction And Electrical Resistivity Tomograms, Electronic Theses and Dissertations. 433. https://egrove.olemiss.edu/etd/433
Zelt, C. A. 2010, Seismic refraction shootout: blind test of methods for obtaining velocity models from first-arrival travel times, http://terra.rice.edu/department/faculty/zelt/sageep2011.
Zelt, C.A., Haines, S., Powers, M.H. et al. 2013, Blind Test of Methods for Obtaining 2-D Near-Surface Seismic Velocity Models from First-Arrival Traveltimes, JEEG, Volume 18(3), 183-194.
Zelt, C. A., Chen, J., 2016, Frequency-dependent traveltime tomography for near-surface seismic refraction data, Geophys. J. Int., Volume 207, 72-88.

Acknowledgements

We thank Dr. Leti Wodajo at Univ. of Mississippi for sharing above data and background information and for his review of this short tutorial.

Copyright © 1996-2021 Intelligent Resources Inc. Some rights reserved.